PROCEEDINGS OF SCIENCE

Photon-photon fusion and $(g-2)_\tau$ measurement at the ATLAS experiment

Kristof Schmieden[a,*] **on behalf of the ATLAS Collaboration**

[a] *Johannes Gutenberg Universität, Mainz, Germany*

E-mail: kristof.schmieden@cern.ch

High statistics measurements of light-by-light scattering, made accessible using relativistic heavy-ion beams provide a precise and unique opportunity to investigate extensions of the Standard Model, such as the presence of axion-like particles. The corresponding measurement of the ATLAS Collaboration is discussed as well as the study of exclusive dilepton production (electron, muon, and tau pairs) in photon-photon fusion. Furthermore, the tau-pair production measurements are used to constrain the tau lepton's anomalous magnetic dipole moment.

ATL-PHYS-PROC-2023-002
22 January 2023

8th Symposium on Prospects in the Physics of Discrete Symmetries (DISCRETE 2022)
7-11 November, 2022
Baden-Baden, Germany

*Speaker

PoS(DISCRETE2022)062

1. Introduction

With the development of Dirac's theory and the discovery of anti-particles in the early 1930s it became evident that photons could scatter off each other. This process, forbidden in classical electrodynamics, is mediated via the box-diagram shown in Figure 1 (left) at order α_{em}^4, where α_{em} is the fine-structure constant. It took more than 80 years until the first direct evidence of the process $\gamma\gamma \to \gamma\gamma$ was seen by the ATLAS [1], [2] and CMS collaborations [3], [4], followed by the observation of this process in 2019 [5]. Any particle directly coupling to two photons may contribute to the photon-photon scattering cross section via an S-channel process, shown in Figure 1 (middle). This includes pseudo-scalar mesons like π^0 and η, η' which are too light to be experimentally observed in $\gamma\gamma$ scattering. More interestingly, any new pseudo-scalar particle like the hypothetical axion like particles (ALPs) would also contribute this process. Using heavy ion (HI) beams to study light-by-light scattering at the LHC was first proposed in Ref. [6]. These events are a superb way to search for ALPs as first proposed in Ref. [7].

Another interesting process is the exclusive production of di-lepton pairs in photon fusion processes, as shown in Figure 1 (right). Of particular interest is the sensitivity to the anomalous magnetic moment of τ-leptons (a_τ) as presented in [8] and recently measured by ATLAS [9], while previously measured by the DELPHI collaboration in 2004 [10] with a precision of 5%.

This paper is structured as follows. After discussing the LHC as photon collider in section 2 the search for ALPs in $\gamma\gamma$ scattering events is discussed in section 3. The measurement of lepton pair production in photon fusion events and the measurement of the anomalous magnetic moment of the τ is presented in section 4.

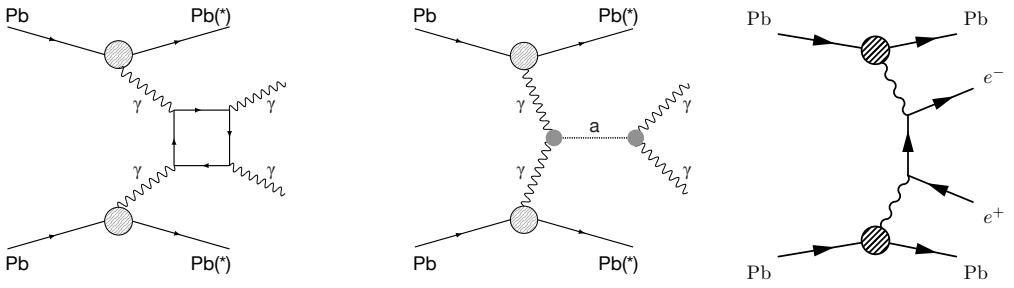

Figure 1: Feynman diagrams showing photon fusion processes [11], [12]. Left: $\gamma\gamma \to \gamma\gamma$ mediated via a box-diagram. Middle: S-channel production of a pseudo-scalar axion like particle (ALP). Right: Di-lepton production.

2. The LHC as photon collider

The relativistic heavy ion beams of the LHC provide an intense source of high energy photons. The electromagnetic (EM) field of relativistic charged particles can be equivalently described as a flux of quasi-real photons [13]. As the photon flux scales with the charge of the beam particles to the power of four, Pb ion beams produce a larger photon flux compared to the proton beams, despite their lower instantaneous luminosity. Additionally, the low luminosity of Pb+Pb collisions with an average number of simultaneous Pb+Pb collisions smaller than one (i.e. pileup-free) leads to very

clean events. Whenever the Pb nuclei do not collide, the surrounding photon fields may still interact while the Pb nuclei stay intact. Those interactions are called ultra peripheral collisions (UPC) and are exploited in the presented measurements. This is only possible as the Pb+Pb collisions are pileup-free in contrast to pp collisions where the average number of simultaneous interactions is about 50. Pileup prevents the identification of $\gamma\gamma$ collision without tagging the scattered protons. Several analyses exploit the ATLAS forward proton tagger (AFP) to tag the scattered protons [14], [15]. However, they are sensitive in a different area of phase space due to the usage of the proton tagger and are not discussed in this paper.

The maximum energy of the photons is given by the Lorentz boost of the beam particles divided by their radius γ/R and is about 80 GeV for Pb beams at 2.51 TeV energy per nucleon. Both the photon flux as well as the $\gamma\gamma$ cross section are exponentially falling with increasing photon energy. Hence it is desirable to study low momentum final state particles.

The LHC is usually operating 4 weeks per year with Pb beams and is expected to triple the available statistics during run-3 of the LHC.

3. Searching for axion like particles

Axions were postulated by Peccei and Quinn [16] in 1977 as a solution to the so called *strong CP problem* [17], [18] of quantum chromo dynamics. They obey a well-defined relation between their mass and coupling to SM particles. Dropping the mass – coupling relation, any scalar or pseudo-scalar particle with similar couplings to SM particles may be referred to as *axion-like* particle (ALP). While axions are generally expected to be very light in the sub-eV regime, masses of ALPs are not constraint. ALPs are predicted in several extensions of the standard model (SM). Most notably they appear in supersymmetrical and, more generally, in any model based on string theory where axions appear through the compactification process of extra dimensions [19]. As ALPs may have very small couplings to SM particles they are an excellent candidate for dark matter. Since several years now these properties made axions very popular particles and many studies are underway to look for them. At the LHC, ALP masses from MeV to hundreds of GeV are accessible via various production and decay modes. Of particular interest is the production via $\gamma\gamma$ fusion as ALPs are expected to couple to photon. In addition this production channel provides a very clean signature as long as no pileup is present.

ALPs may decay into a variety of particles. At the LHC final states with photons, muons, tauons and b-quarks as well as invisible decays are currently studied. The decay into photons is experimentally clean and of particular interest in combination with the production via photon-photon fusion and is described in the following. For an overview of studies covering alternative production and decay modes see e.g. [20].

3.1 ALPs in photon–photon collisions

At the LHC the search for ALPs in photon collisions is of particular interest due to its uniquely clean signature of the $\gamma\gamma \to a \to \gamma\gamma$ process, which would show up as a peak in the invariant di-photon mass spectrum over the continuous SM light-by-light scattering background. These analyses use data from ultra-peripheral heavy ion collisions.

The ATLAS analysis is published in Ref. [11]. Candidate events are selected by requiring exactly two photons above a low energy threshold in the detector and vetoing any additional activity. The photons are required to be back-to-back in the axial plane of the detector to suppress background from gluon-gluon fusion events as well as from electron-positron pairs misidentified as photons. Using 2.2 nb^{-1} of Pb+Pb data recorded in 2015 and 2018 ATLAS identified 97 candidate events of the $\gamma\gamma$ scattering process. This results in a measured cross section of $120 \pm 17(stat) \pm 13(sys) \pm 4(lumi)$ nb, compared to a predicted cross section of 78 ± 8 nb [21]. An ALP signal would appear as narrow peak in the di-photon invariant mass spectrum. The resulting invariant mass spectrum, which is shown in Figure 2 (left). As no signal is observed limits on the ALP coupling to photons are set in the full mass range from 5 GeV to 100 GeV and presented in Figure 2 (right). Those are the most stringent limits in the mass range from 5 GeV to 30 GeV to date.

CMS also measured this process and calculated limits on the coupling of ALPs to photons presented in Ref. [4].

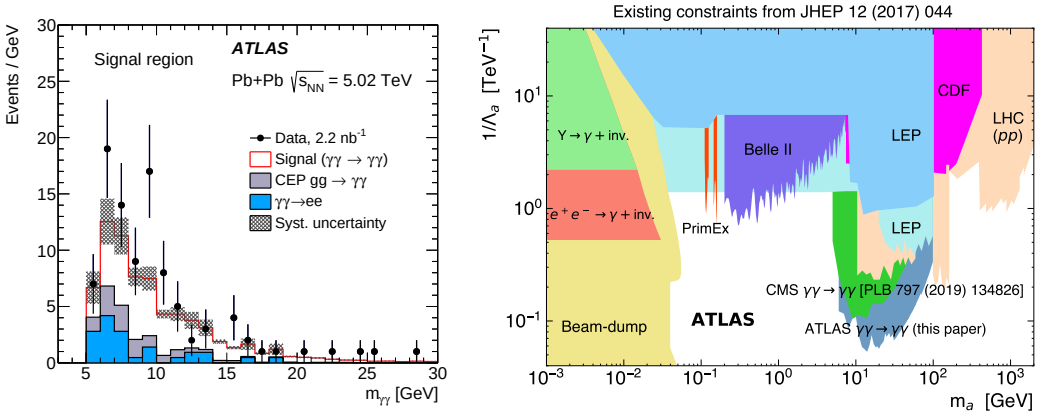

Figure 2: Left: Invariant mass spectrum of the measured $\gamma\gamma$ scattering events in comparison to the simulated signal process and background prediction. Right: Derived limits on the coupling of axion like particles to photons [11].

4. Measurement of the anomalous magnetic moment of the tauon

Measurements of the anomalous magnetic moment, $a_l = \frac{1}{2}(g_l - 2)$, of charged leptons l (electrons, muons, and τ-leptons) are cornerstone tests of the standard model with unique sensitivity to beyond- the-SM phenomena. The leading contribution to a_l in the SM is the one-loop Schwinger term $\alpha_{\text{em}}/2\pi \approx 0.00116$ [22], [23], where α_{em} is the electromagnetic fine-structure constant. For the electron (muon), a_e (a_μ) is tested to parts per 10^{10} [24], [25](10^7 [26], [27]) precision while a_τ is only measured to about 5% [28]. Measurements of a_μ report tensions with the SM expectation [29]–[32], which may suggest BSM dynamics. Specific BSM scenarios such as supersymmetry [33] predict enhancements that scale quadratically with the lepton mass resulting in a $(m_\tau/m_\mu)^2 \approx 280$ times larger effect for τ-leptons. However, the short τ-lepton lifetime precludes precise spin-precession measurements of a_τ to test the SM prediction of $a_\tau^{\text{SM}} = 0.00117721(5)$ [34] and potential BSM contributions.

ATLAS recently observed the production of di-τ pairs in photon fusion events using UPC events in 1.44nb^{-1} of Pb+Pb data at $\sqrt{S_{NN}} = 5.02$ TeV recorded in 2018 [35]. As τ-leptons may decay into an electron or muon plus additional neutrinos, or one or three additional charged pions, three signal regions are used in the analysis. Exactly one muon is required in each event, i.e. one τ is required to decay into a muon. This reduces the background from $\gamma\gamma \to \mu\mu$ and $\gamma\gamma \to q\bar{q}$ events. The decay of the second τ defines the signal region (SR): μe-SR requires exactly one additional electron and no other tracks. The μ+1 track (μ+3 tracks) SR require exactly one (three) additional tracks separated from the muon by $\Delta R_{\mu,\text{trk}} > 0.1$ which selects one and three prong decays of the second τ-lepton. The signature of the three signal categories is shown in Figure 3. The corresponding Feynman diagrams are shown in Figure 4. The photon initial state is tagged by requiring that no neutron is detected in the zero degree calorimeter (ZDC). This suppresses all processes where the Pb ions would break up, which is the case for photo-nuclear background processes as well as non-UPC events. The dominant sources of background are radiative di-muon ($\gamma\gamma \to \mu\mu\gamma$) and photonuclear processes with low central detector activity. The muon transverse momentum distribution from the selected events is shown for all signal categories in Figure 5 together with the signal and background expectation, where the photonuclear background is estimated from data. A clear signal of the $\gamma\gamma \to \tau\tau$ process is observed. The normalisation of the photon flux is one of the dominant uncertainties. During the fit procedure it is constrained from a dedicated control region selecting predominantly $\gamma\gamma \to \mu\mu$ events. This channel as well as the di-electron production in photon fusion events were previously studied in detail in Refs. [36] and [12].

The $p_\text{T}(\mu)$ distribution is sensitive to the anomalous magnetic moment of the τ as can be seen by the predictions using two different values of a_τ, simulated using the STARLIGHT 2.0 MC generator interfaced with TAUOLA.

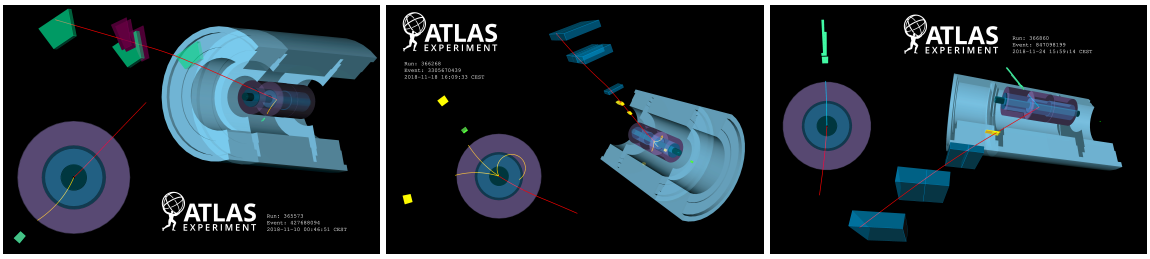

Figure 3: Event displays for exclusive $\gamma\gamma \to \tau\tau$ candidates from the (left) μ1T-SR, (middle) μ3T-SR and (right) μe-SR. Muons are indicated as red line, charged particles as orange lines and the electron as blue line with the calorimeter cluster depicted in green. All calorimeter cells passing the following E_T thresholds are shown: $E_\text{T} > 250$ MeV for the central calorimeters and the electromagnetic end-cap, $E_\text{T} > 800$ MeV for hadronic end-cap calorimeter, and $E_\text{T} > 100$ MeV for the forward calorimeters. All charged-particle tracks with $p_\text{T} > 100$ MeV are shown.

Fitting various predictions of p_T^μ to the measured distribution with a_τ as free parameter yield the best fit value of $a_\tau = -0.041$ with the 95% CL interval covering $a_\tau \in (-0.057, 0.024)$ as shown in Figure 6. The uncertainty is dominated by the statistical uncertainty of the measurement. The precision of this measurement is similar to the most precise single-experiment measurement by the DELPHI Collaboration from 2004 [10].

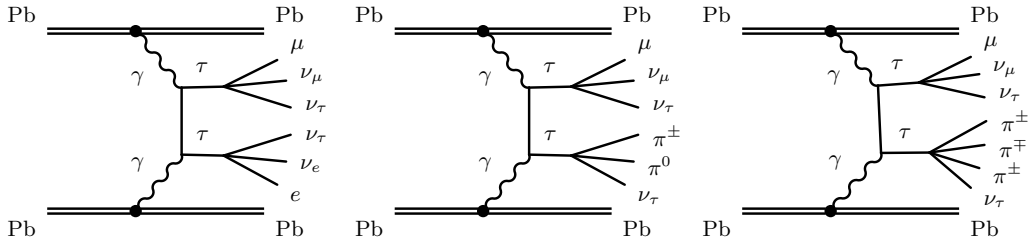

Figure 4: Schematic Feynman diagrams showing photon-induced τ-lepton pair production in ultraperipheral lead-lead interactions, Pb + Pb $\rightarrow$ Pb($\gamma\gamma \rightarrow \tau\tau$)Pb, with the τ-leptons decaying into illustrative signatures targeted by the event selection: (left) one muon and one electron, (centre) one muon and one charged pion $\pi^\pm$, (right) one muon and three charged pions.

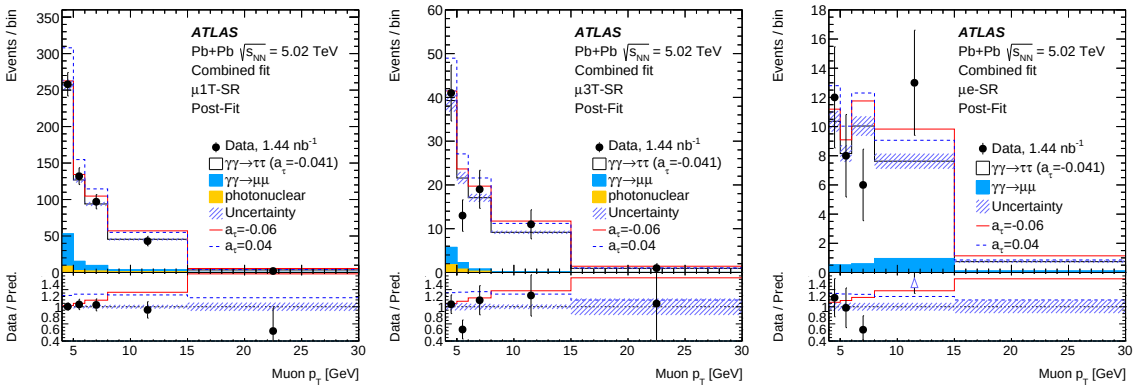

Figure 5: Muon transverse momentum distributions in the (left) μ1T-SR, (middle) μ3T-SR, (right) μe-SR categories. Black markers denote data and stacked histograms indicate the different components contributing to the regions. Post-fit distributions are shown with the signal contribution corresponding to the best-fit a_τ value (a_τ=-0.041). For comparison, signal contributions with alternative a_τ values are shown as solid red ($a_\tau = -0.06$) or dashed blue ($a_\tau = 0.04$) lines. The bottom panel shows the ratio of the data to post-fit predictions. Vertical bars denote uncertainties from the finite number of data events. Hatched bands represent $\pm 1\sigma$ systematic uncertainties of the prediction with the constraints from the fit applied.

5. Conclusions

The LHC proves to be a versatile tool to study high energy photon-photon fusion signatures in ultraperipheral lead-lead collisions. Using photon final states the $\gamma\gamma \rightarrow \gamma\gamma$ process is studied, allowing to search for the production of axion like particles. While no significant excess of events has been observed over the standard model background the most stringent limits to date on the axion-photon coupling could be set in the mass range from 5 GeV to 30 GeV. Investigating leptonic final states the anomalous magnetic moment of the τ-lepton is measured with a precision comparable to that of LEP experiments, dominated by the statistical uncertainty.

The photon fusion processes provide in very sensitive probe of the standard model and have the potential to increase the precision significantly using the expected LHC run-3 data.

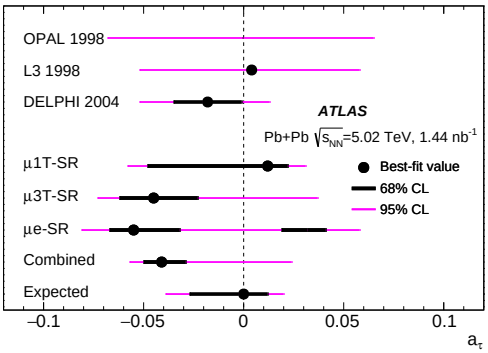

Figure 6: Measurements of the anomalous magnetic moment of the τ-lepton. These fit results in the individual and combined signal regions are compared to existing measurements from the OPAL [37], L3 [38] and DELPHI [10] experiments at LEP. A point denotes the best-fit a_τ value for each measurement if available, while thick black (thin magenta) lines show 68% CL (95% CL) intervals. The expected interval from the ATLAS combined fit is also shown.

References

[1] ATLAS Collaboration, "The ATLAS Experiment at the CERN Large Hadron Collider," *JINST*, vol. 3, S08003, 2008. DOI: 10.1088/1748-0221/3/08/S08003.

[2] ATLAS Collaboration, "Evidence for light-by-light scattering in heavy-ion collisions with the ATLAS detector at the LHC," *Nature Phys.*, vol. 13, p. 852, 2017. DOI: 10.1038/nphys4208. arXiv: 1702.01625 [hep-ex].

[3] CMS Collaboration, "The CMS Experiment at the CERN LHC," *JINST*, vol. 3, S08004, 2008. DOI: 10.1088/1748-0221/3/08/S08004.

[4] CMS Collaboration, "Evidence for light-by-light scattering and searches for axion-like particles in ultraperipheral PbPb collisions at $\sqrt{s_{\mathrm{NN}}} = 5.02\,\mathrm{TeV}$," *Phys. Lett. B*, vol. 797, p. 134 826, 2019. DOI: 10.1016/j.physletb.2019.134826. arXiv: 1810.04602 [hep-ex].

[5] ATLAS Collaboration, "Observation of Light-by-Light Scattering in Ultraperipheral Pb+Pb Collisions with the ATLAS Detector," *Phys. Rev. Lett.*, vol. 123, p. 052 001, 2019. DOI: 10.1103/PhysRevLett.123.052001. arXiv: 1904.03536 [hep-ex].

[6] D. d'Enterria and G. G. da Silveira, "Observing light-by-light scattering at the large hadron collider," *Phys. Rev. Lett.*, vol. 111, p. 080 405, 8 2013. DOI: 10.1103/PhysRevLett.111.080405.

[7] S. Knapen, T. Lin, H. K. Lou, and T. Melia, "Searching for Axionlike Particles with Ultraperipheral Heavy-Ion Collisions," *Phys. Rev. Lett.*, vol. 118, no. 17, p. 171 801, 2017. DOI: 10.1103/PhysRevLett.118.171801. arXiv: 1607.06083 [hep-ph].

[8] M. Dyndal, M. Klusek-Gawenda, M. Schott, and A. Szczurek, "Anomalous electromagnetic moments of τ lepton in $\gamma\gamma \to \tau^+\tau^-$ reaction in Pb+Pb collisions at the LHC," *Phys. Lett. B*, vol. 809, p. 135 682, 2020. DOI: 10.1016/j.physletb.2020.135682. arXiv: 2002.05503 [hep-ph].

[9] "Observation of the $\gamma\gamma \to \tau\tau$ process in Pb+Pb collisions and constraints on the τ-lepton anomalous magnetic moment with the ATLAS detector," 2022. arXiv: 2204.13478 [hep-ex].

[10] J. Abdallah *et al.*, "Study of tau-pair production in photon-photon collisions at LEP and limits on the anomalous electromagnetic moments of the tau lepton," *Eur. Phys. J. C*, vol. 35, pp. 159–170, 2004. DOI: 10.1140/epjc/s2004-01852-y. arXiv: hep-ex/0406010.

[11] ATLAS Collaboration, "Measurement of light-by-light scattering and search for axion-like particles with 2.2 nb^{-1} of Pb+Pb data with the ATLAS detector," *JHEP*, vol. 03, p. 243, 2021. DOI: 10.1007/JHEP03(2021)243. arXiv: 2008.05355 [hep-ex], Erratum: *JHEP*, vol. 11, p. 050, 2021. DOI: 10.1007/JHEP11(2021)050.

[12] ATLAS Collaboration, "Exclusive dielectron production in ultraperipheral Pb+Pb collisions at $\sqrt{s_{\mathrm{NN}}} = 5.02$ TeV with ATLAS," 2022. arXiv: 2207.12781 [nucl-ex].

[13] E. J. Williams, "Nature of the high energy particles of penetrating radiation and status of ionization and radiation formulae," *Phys. Rev.*, vol. 45, pp. 729–730, 10 1934. DOI: 10.1103/PhysRev.45.729.

[14] ATLAS Collaboration, "Observation and Measurement of Forward Proton Scattering in Association with Lepton Pairs Produced via the Photon Fusion Mechanism at ATLAS," *Phys. Rev. Lett.*, vol. 125, p. 261 801, 2020. DOI: 10.1103/PhysRevLett.125.261801. arXiv: 2009.14537 [hep-ex].

[15] ATLAS Collaboration, "Observation of photon-induced W^+W^- production in pp collisions at $\sqrt{s} = 13$ TeV using the ATLAS detector," *Phys. Lett. B*, vol. 816, p. 136 190, 2021. DOI: 10.1016/j.physletb.2021.136190. arXiv: 2010.04019 [hep-ex].

[16] R. D. Peccei and H. R. Quinn, "CP Conservation in the presence of pseudoparticles," *Phys. Rev. Lett.*, vol. 38, pp. 1440–1443, 25 1977. DOI: 10.1103/PhysRevLett.38.1440.

[17] S. Weinberg, "A new light boson?" *Phys. Rev. Lett.*, vol. 40, pp. 223–226, 4 1978. DOI: 10.1103/PhysRevLett.40.223.

[18] F. Wilczek, "Problem of strong P and T invariance in the presence of instantons," *Phys. Rev. Lett.*, vol. 40, pp. 279–282, 5 1978. DOI: 10.1103/PhysRevLett.40.279.

[19] P. Svrcek and E. Witten, "Axions In String Theory," *JHEP*, vol. 06, p. 051, 2006. DOI: 10.1088/1126-6708/2006/06/051. arXiv: hep-th/0605206.

[20] K. Schmieden, "Searches for Axion Like Particles at the LHC," *PoS*, vol. LHCP2021, p. 005, 2021. DOI: 10.22323/1.397.0005.

[21] L. A. Harland-Lang, V. A. Khoze, and M. G. Ryskin, "Exclusive LHC physics with heavy ions: SuperChic 3," *Eur. Phys. J. C*, vol. 79, no. 1, p. 39, 2019. DOI: 10.1140/epjc/s10052-018-6530-5. arXiv: 1810.06567 [hep-ph].

[22] J. Schwinger, "On quantum-electrodynamics and the magnetic moment of the electron," *Phys. Rev.*, vol. 73, pp. 416–417, 4 1948. DOI: 10.1103/PhysRev.73.416.

[23] P. Kusch and H. M. Foley, "The magnetic moment of the electron," *Phys. Rev.*, vol. 74, pp. 250–263, 3 1948. DOI: 10.1103/PhysRev.74.250.

[24] B. Odom, D. Hanneke, B. D'Urso, and G. Gabrielse, "New measurement of the electron magnetic moment using a one-electron quantum cyclotron," *Phys. Rev. Lett.*, vol. 97, p. 030 801, 3 2006. DOI: 10.1103/PhysRevLett.97.030801.

[25] L. Morel, Z. Yao, P. Cladé, and S. Guellati-Khelifa, "Determination of the fine-structure constant with an accuracy of 81 parts per trillion," *Nature*, vol. 588, pp. 61–65, 2020. DOI: 10.1038/s41586-020-2964-7.

[26] G. W. Bennett *et al.*, "Final Report of the Muon E821 Anomalous Magnetic Moment Measurement at BNL," *Phys. Rev. D*, vol. 73, p. 072 003, 2006. DOI: 10.1103/PhysRevD.73.072003. arXiv: hep-ex/0602035.

[27] T. Albahri *et al.*, "Measurement of the anomalous precession frequency of the muon in the Fermilab Muon $g-2$ Experiment," *Phys. Rev. D*, vol. 103, no. 7, p. 072 002, 2021. DOI: 10.1103/PhysRevD.103.072002. arXiv: 2104.03247 [hep-ex].

[28] M. Tanabashi, K. Hagiwara, K. Hikasa, *et al.*, "Review of particle physics," *Phys. Rev. D*, vol. 98, p. 030 001, 3 2018. DOI: 10.1103/PhysRevD.98.030001.

[29] T. Aoyama, M. Hayakawa, T. Kinoshita, and M. Nio, "Complete Tenth-Order QED Contribution to the Muon g-2," *Phys. Rev. Lett.*, vol. 109, p. 111 808, 2012. DOI: 10.1103/PhysRevLett.109.111808. arXiv: 1205.5370 [hep-ph].

[30] T. Aoyama *et al.*, "The anomalous magnetic moment of the muon in the Standard Model," *Phys. Rept.*, vol. 887, pp. 1–166, 2020. DOI: 10.1016/j.physrep.2020.07.006. arXiv: 2006.04822 [hep-ph].

[31] M. Davier, A. Hoecker, B. Malaescu, and Z. Zhang, "A new evaluation of the hadronic vacuum polarisation contributions to the muon anomalous magnetic moment and to $\alpha(\mathbf{m_Z^2})$," *Eur. Phys. J. C*, vol. 80, no. 3, p. 241, 2020, [Erratum: Eur.Phys.J.C 80, 410 (2020)]. DOI: 10.1140/epjc/s10052-020-7792-2. arXiv: 1908.00921 [hep-ph].

[32] S. Borsanyi *et al.*, "Leading hadronic contribution to the muon magnetic moment from lattice QCD," *Nature*, vol. 593, no. 7857, pp. 51–55, 2021. DOI: 10.1038/s41586-021-03418-1. arXiv: 2002.12347 [hep-lat].

[33] S. P. Martin and J. D. Wells, "Muon Anomalous Magnetic Dipole Moment in Supersymmetric Theories," *Phys. Rev. D*, vol. 64, p. 035 003, 2001. DOI: 10.1103/PhysRevD.64.035003. arXiv: hep-ph/0103067.

[34] S. Eidelman and M. Passera, "Theory of the tau lepton anomalous magnetic moment," *Mod. Phys. Lett. A*, vol. 22, pp. 159–179, 2007. DOI: 10.1142/S0217732307022694. arXiv: hep-ph/0701260.

[35] ATLAS Collaboration, "Observation of the $\gamma\gamma \to \tau\tau$ process in Pb+Pb collisions and constraints on the τ-lepton anomalous magnetic moment with the ATLAS detector," 2022. arXiv: 2204.13478 [hep-ex].

[36] ATLAS Collaboration, "Exclusive dimuon production in ultraperipheral Pb+Pb collisions at $\sqrt{s_{\mathrm{NN}}} = 5.02$ TeV with ATLAS," *Phys. Rev. C*, vol. 104, p. 024 906, 2020. DOI: 10.1103/PhysRevC.104.024906. arXiv: 2011.12211 [hep-ex].

[37] K. Ackerstaff *et al.*, "An Upper limit on the anomalous magnetic moment of the tau lepton," *Phys. Lett. B*, vol. 431, pp. 188–198, 1998. DOI: 10.1016/S0370-2693(98)00520-6. arXiv: hep-ex/9803020.

[38] M. Acciarri, O. Adriani, M. Aguilar-Benitez, *et al.*, "Measurement of the anomalous magnetic and electric dipole moments of the tau lepton," *Physics Letters B*, vol. 434, no. 1, pp. 169–179, 1998, ISSN: 0370-2693. DOI: https://doi.org/10.1016/S0370-2693(98)00736-9.